

pubs.acs.org/journal/abseba Article

Reduced Biofilm Formation at the Air—Liquid—Solid Interface via Introduction of Surfactants

Pengyu Chen, Jiayan Lang, Trevor Donadt, Zichen Yu, and Rong Yang*



Cite This: https://doi.org/10.1021/acsbiomaterials.0c01691



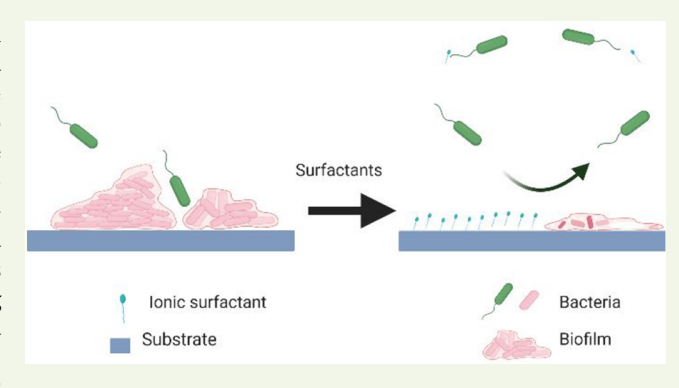
ACCESS

Metrics & More



Supporting Information

ABSTRACT: Reduced biofilm formation is highly desirable in applications ranging from transportation to separations and healthcare. Biofilms often form at the three-phase interface where air, liquid, and solid coexist due to the close proximity to nutrients and oxygen. Reducing biofilm formation at the triple interface presents challenges because of the conflicting requirements for hydrophobicity at the air—solid interface (for self-cleaning properties) and for hydrophilicity at the liquid—solid interface (for reduced foulant adhesion). Meeting those needs simultaneously likely entails a dynamic surface, capable of shifting the surface energy landscape in response to wetting conditions and thus enabling hydrophobicity in air and hydrophilicity in water. Here, we designed a facile approach to render existing surfaces



resistant to biofilm formation at the triple interface. By adding trace amounts (~0.1 mM) of surfactants, biofilm formation of *Pseudomonas aeruginosa* (known to form biofilm at the triple interface) was reduced on all surfaces tested, ranging from hydrophilic to hydrophobic, polar to nonpolar. That reduced fouling was not a result of the known antimicrobial effects. Instead, it was attributed to the surface-adsorbed surfactants that dynamically control surface energy at the triple interface. To further understand the effect of surfactant–surface interactions on biofilm reduction, we systematically varied the surfactant charge type and surface properties (surface energy and charge). Electrostatic interactions between surfactants and surfaces were identified as an influential factor when predicting the relative fouling reduction upon introduction of surfactants. Nevertheless, biofilm formation was reduced even on the charge-neutral, fluorinated surface made of poly(1H, 1H, 2H, 2H-perfluorodecyl acrylate) by more than 2-fold simply via adding 0.2 mM dodecyl trimethylammonium chloride or 0.3 mM sodium dodecyl sulfate. Given its robustness, this strategy is broadly applicable for reducing fouling on existing surfaces, which in turn improves the cost-effectiveness of membrane separations and mitigates contaminations and nosocomial infections in healthcare.

KEYWORDS: antifouling, three-phase interface, polymer coating, biofilm, surfactant, initiated chemical vapor deposition

■ INTRODUCTION

Biofouling, the nonspecific attachment of organic molecules and living organisms onto submerged surfaces, causes severe contamination, energy inefficiency, and material degradation in marine transportation, healthcare, and membrane separation. Current antifouling strategies have predominantly focused on the development of new materials, ones that could deter or even prevent nonspecific surface binding. Enhancing surface hydrophilicity is by far the most effective strategy in antifouling material design, which led to the implementation of ultralow fouling zwitterionic chemistry. Despite their success in reducing fouling on fully submerged surfaces, existing antifouling chemistries have rarely been proven effective at the air—liquid—solid interface, where severe fouling is known to occur. Strategy in the context of the co

Fouling resistance at the triple interface likely requires strategies that are distinct from those developed for fully submerged surfaces. While strong hydration is favorable for antifouling properties at the liquid—solid interface, the opposite is true for the air—solid interface. Self-cleaning surfaces, ones that remain clean under ambient, dry conditions often rely on their hydrophobicity to enable water droplets to roll off the surface, carrying away contaminants. A dynamic surface that presents hydrophobicity in air but becomes hydrophilic upon wetting is likely required to satisfy the seemingly conflicting requirements for antifouling at the liquid—solid versus air—solid interfaces. We hypothesized that introducing small-molecule ionic surfactants into the

Special Issue: Engineering Bioinspired and Biological

Materials

Received: December 3, 2020 Accepted: March 30, 2021



liquid system in trace amounts could render existing surfaces dynamic, without the need to redesign surface properties.

At concentrations below the critical micelle concentration (CMC), small-molecule ionic surfactants tend to partition toward an interface to reduce the free energy of the system, leaving their presence sparse in the bulk liquid phase. On the molecular level, ionic surfactants are known to interact with solid surfaces via electrostatic and/or van der Waals interactions, forming oriented monolayers or hemimicelle structures at the fluid-solid interface. When submerged, the surface-concentrated surfactants adopt a configuration to maximize the exposure of hydrophilic head groups while directing tightly packed alkyl tails toward the solid surface. 10-12 Under ambient conditions, the hydrophobic tails are oriented toward the air-solid interface to minimize the interfacial energy, creating a hydrophobic surface. Our design capitalized on that dynamic behavior to achieve simultaneous fouling reduction at the liquid-solid and air-solid interfaces.

To further understand the effect of surfactant-surface interactions on biofilm reduction, we systematically varied the surfactant charge type and the properties of an existing surface. Specifically, the effect of surfactant charge type was illustrated using the anionic surfactant sodium dodecyl sulfate (SDS, CMC = 6.7 mM) and cationic surfactant dodecyl trimethylammonium chloride (DTAC, CMC = 14.6 mM), both with an identical 12-carbon aliphatic tail. ¹³ Biofilm formation at the triple interface was reduced by 1.0-3.6-fold by adding 0.1 mM SDS, and 2.2-10.2-fold by adding 0.1 mM DTAC. The dynamic interactions between the surfactants and an existing surface were unraveled by varying properties of the surface including surface energy, functional moieties, and charge. Specifically, polyvinyl chloride (PVC) surfaces were coated with zwitterionic polymer (ZWP), poly(2-hydroxyethyl methacrylate) (PHEMA), and poly(1H,1H,2H,2H-perfluorodecyl acrylate) (PPFDA) respectively, which represent varying degrees of surface hydrophilicity, hydrophobicity, charge, and functional moieties relevant to antifouling applications. The greatest reduction in biofilm formation at the triple interface (by 10.2-fold) was observed on PHEMA when 0.1 mM DTAC was added, which was attributed to the strong electrostatic interactions between the negatively charged PHEMA surface and cationic surfactant. The 10.2-fold fouling reduction on PHEMA was a notable improvement given the known fouling resistance of PHEMA.12

Although small-molecule antimicrobials have been used in the solution phase to kill bacteria or prevent them from forming biofilms, ^{15–20} the reduced fouling observed here was not a result of the known antimicrobial effects of surfactants. ²¹ In the presence of 0.1 mM surfactants, growth of *P. aeruginosa* remained unchanged, which was corroborated by the confocal images of the biofilms. Nevertheless, the low-concentration surfactants changed the morphology of biofilms from a continuous film of extracellular matrix into a porous structure with exposed cells. That structural disruption is a potential reason for the reduced biofilm formation on the solid surfaces. ²² Further reduction of biofilm formation at the triple interface could be achieved up to 10-fold by increasing the concentration of surfactants.

The facile approach of introducing trace amounts of surfactants represents a cost-effective strategy to reduce biofilm formation at the triple interface for a large variety of surface chemistries. It highlights the important consideration of interfacial adsorption of small, ionic molecules during the

design and development of antifouling strategies. The approach has direct applications in membrane separation for water purification and environmental sustainability, where surfactants could be introduced to the feed side (e.g., of reverse osmosis processes) to reduce fouling without causing pollution of the permeate. Furthermore, the surfactant—surface interactions reported here could inform the design of antifouling surfaces in healthcare, transportation, and manufacturing.

EXPERIMENTAL SECTION

Initiated Chemical Vapor Deposition (iCVD). All of the polymeric surfaces were created using iCVD technology in a custombuilt cylindrical vacuum reactor (Sharon Vacuum Co Inc., Brockton, MA, USA). Thermal excitation of the initiators was provided by heating a 0.5 mm nickel/chromium filament (80% Ni/20% Cr, Goodfellow) mounted as a parallel filament array. Filament temperature was controlled by a feedback loop, whose reading came from a thermocouple attached to one of the filaments. The filament holder straddled the deposition stage that was kept at desired substrate temperatures using a chiller. The vertical distance between the filament array and the stage was ~2 cm. Depositions were performed on two kinds of substrates: Si wafers (P/Boron <100>, Purewafer, San Jose, CA, USA) and 96-well microplates (Clear Round Bottom Polyvinyl Chloride (PVC) Non-Treated Microplate, Corning). Cooling of the latter was further enhanced by a custom-designed aluminum holder. Initiator (tert-butyl peroxide (TBPO, Sigma-Aldrich, 98%)) and monomers (2-hydroxyethyl methacrylate (Sigma-Aldrich, ≥ 99%), 4-vinylpyridine (4VP, Sigma-Aldrich, 95%), divinylbenzene (DVB, Sigma-Aldrich, 80%), and 1H,1H,2H,2H-perfluorodecyl acrylate (PFDA, Sigma-Aldrich, 97%) were used without further purification. During the iCVD depositions, TBPO and argon patch flow were fed to the reactor at room temperature through mass flow controllers at 0.6 sccm and desired flow rates (see below, deposition parameters), respectively. HEMA, 4VP, DVB, and PFDA were heated to 70, 60, 65, and 80 °C in glass jars, respectively, to create sufficient pressure to drive vapor flow. Films were deposited at a filament temperature of 220 °C. The total pressure of the chamber was controlled by a butterfly valve. In situ interferometry with a HeNe laser source (wavelength = 633 nm, IDS Uniphase) was used to monitor the film growth on a Si substrate. The deposition parameters are listed below:

During the PHEMA depositions, flow rate of HEMA was 0.2 sccm. The argon flow rate was 1.5 sccm. The total flow rate was 2.3 sccm. The stage temperature was set to be 20 °C. The chamber pressure was 350 mTorr. Under those conditions, the $P_{\rm M}/P_{\rm M}^{\rm sat}$ (the ratio of partial pressure of monomer to the saturated pressure under the stage temperature) of HEMA was 0.29.

During the PPFDA depositions, flow rate of PFDA was 0.2 sccm. The argon flow rate was 2.0 sccm. The total flow rate was 2.8 sccm. The stage temperature was set to be 30 °C. The chamber pressure was 400 mTorr. Under those conditions, the $P_{\rm M}/P_{\rm M}^{\rm sat}$ of PPFDA was 0.38.

During the P4VP-DVB depositions, the flow rate of 4VP was 3.0 sccm. Due to the high solubility of the zwitterionic polymer, we introduced DVB as a cross-linker to prevent the derivatized film from dissolving. The flow rate of DVB was 0.1 sccm. The total flow rate was 3.7 sccm. The stage temperature was set to be 20 °C. The chamber pressure was 500 mTorr. Under these conditions, the value of $P_{\rm 4VP}/P_{\rm 54V}^{\rm sat}$ was 0.33, the value of $P_{\rm DVB}/P_{\rm DVB}^{\rm sat}$ was 0.027. In a second step, the coated substrates were fixed in a crystallizing dish (VWR) with 1 g of 1,3-propane sultone (Sigma-Aldrich, 98%). The crystallizing dish was placed inside a vacuum oven that was maintained at 25 Torr and 75 °C for 12 h to allow the 1,3-propane sultone vapor to react with the P4VP-co-DVB coating.

Polymer Film Characterization. Fourier transform infrared (FTIR) measurements were performed on a Bruker Vertex V80v vacuum FTIR system in transmission mode. A deuterated triglycine sulfate (DTGS) KBr detector over the rage of 400–4000 cm⁻¹ was adopted with a resolution of 4 cm⁻¹. The measurements were averaged over 64 scans to obtain a sufficient signal-to noise ratio. All

the spectra were collected on Si wafer coated with polymer thin films and baseline corrected after subtracting a background spectrum of Si wafer without coating.

During XPS, samples were analyzed using a Scienta Omicron ECSA 2SR spectrometer with operating pressure ca. 1×10^{-9} Torr. Monochromatic Al K α X-rays were generated at 300 W (15 kV; 20 mA) with a 2 mm diameter analysis spot. A hemispherical analyzer determined electron kinetic energy, using a pass energy of 200 eV for wide/survey scans, and 50 eV for high resolution scans. A flood gun was used for charge neutralization of nonconductive samples. Data analysis was conducted by CasaXPS with Shirley as the background. All the samples were stored under vacuum at room temperature for a week before XPS analysis.

Biofilm Formation Test. *Pseudomonas aeruginosa (PAO1, ATCC)* was used as the model microorganism. Bacteria cells from -80 °C freezer stocks were scratched on a TSA plate. The plate was placed in an incubator (37 °C) overnight until single colonies formed. A single colony was picked and inoculated into lysogeny broth (LB) medium. The inoculated medium was incubated overnight at 37 °C to stationary phase in a shaker (225 rpm). The overnight suspension was diluted 100 times in fresh LB medium and incubated at 37 °C on a shaker (225 rpm) until the optical density reached 0.2. Surfactants were added into the bacterial suspension until the concentration reached the desired value. 150 μL bacterial suspension was then added into each well of the surface-modified 96-well microplate. The microplates were incubated (37 °C) for 24 h to make sure biofilms were mature. After biofilm formation, the liquid culture and loosely attached bacteria were removed from each well by vigorously washing each well 3-4 times with deionized water (dH₂O). Biofilms were then stained by 175 µL of dH₂O with 0.1 wt % crystal violet for 10 min. The crystal violet solution was then removed by washing each well 3-5 times until the liquid in each well became a clear solution. The microplate was dried in the air at room temperature for 24 h to remove residual water in each well. The biofilm formed was subsequently quantified. Two-hundred microliters of acetic acid solution (30 v/v) was added into each well to release the absorbed crystal violet and the relative amount of absorbed crystal violet was quantified spectrophotometrically by measuring the OD₅₇₀ using a microplate reader (Infinite M1000 Pro, Tecan).

Growth Curve. The aforementioned procedure for biofilm formation was followed during the preparation of bacterial suspensions with a desired concentration of surfactants. 200 μ L of the bacterial suspension was added into a flat-bottom 96-well microplate. The microplate was placed into the microplate reader to incubate at 37 °C. The incubating condition was composed of 30 s of orbital shaking (220 rpm) followed by no movement for 120 s. The OD₆₀₀ was measured every 5 min.

SEM Imaging of Biofilms. Biofilm samples were treated with 0.05 M cacodylate buffer containing 2% glutaraldehyde and 1% osmium tetroxide for fixation. Samples were then dehydrated using critical point drying. The SEM images were obtained using Zeiss Gemini 500 with an acceleration voltage of 3 kV. Carbon was sputter coated onto all samples prior to imaging.

Confocal Imaging of Biofilms. Soda-lime glass slides were used as the substrate during confocal imaging. Slides were cut into 15×10 mm pieces and fixed on the lid of a 12-well microplate (Transparent flat bottom, Corning, NY, USA). The lid, with slides attached, was subsequently rinsed using 70 vol % ethanol and dried in a biosafety cabinet with ultraviolet light irradiation for 30 min before incubation. PAO1 was cultured for 24 h in LB medium at 37 $^{\circ}\text{C}$ in the microplate wells. Biofilm formed near the three-phase boundary (air, culture liquid, glass slide). After incubation, slides were washed twice with PBS buffer. The biofilms were stained by BacLight LIVE/DEAD stain (3 μ L component A + 3 μ L component B per mL of PBS buffer) at room temperature for 15 min. The stained biofilm was then washed twice gently by PBS buffer and fixed by neutral buffered formalin for 30 min at room temperature. The fixative was removed by rinsing with PBS buffer twice. The sample was covered by a coverslip before imaging. To protect the biofilm from deformation caused by coverslip, we used a press-to-seal silicone isolator (8-well, Electron Microscopy

Sciences) to create a 0.5 mm gap between the coverslip and glass slide (where biofilms resided).

Confocal laser scanning microscopy was carried out using Zeiss LSM 710 equipped with 10× water immersion objective and acquired images were analyzed in Zen 3.1 Blue. To acquire SYTO 9 signals, a 488 nm laser and 500–570 nm emission filter was used. For propidium iodide (PI) signals, a 561 nm laser and 605–690 nm emission filter were used. Similar experimental conditions were adopted in different samples to objectively compare the live/dead ratio.

Zeta Potential. Zeta potential was measured on a Zeta Potential Analyzer (Beckman Coulter, USA). To determine the surface zeta potential, the polymer coated glass slide was tested three times with a Flat Surface Cell at 25 °C. The cell constant was measured with a 100 mM NaCl standard solution. To control the pH level at 7, an Auto Titrator was connected to the Flat Surface Cell. The Auto Titrator controlled the pH level to within 0.05 of the target levels and pumped the solution through the cell.

Contact Angle. Contact angle measurements were performed using a Rame-Hart Model 500 goniometer equipped with an automated water dispenser. Static contact angle measurements were recorded using a 5 μ L droplet dispensed upon silicon wafers coated with the polymer thin films or upon flat surfaces of uncoated PVC culture plates.

■ RESULT AND DISCUSSION

At concentrations below the CMC, ionic surfactant molecules are known to partition toward the liquid—solid interface to minimize the overall surface energy. That preferential partition is mediated via electrostatic and/or dispersive forces between surfactants and surfaces. On the molecular level, surfactant molecules could form monolayers or local aggregates, like hemimicelles, at the liquid—solid interface, leading to much higher surface concentration than that of the bulk solution. Depending on the wetting state of the surface, the surfactant layers could rapidly switch between a hydrophobic state, by exposing the hydrophobic tail, and a hydrophilic state, by reorienting the hydrophilic head toward the interface. That dynamic behavior serves as the basis for our design of the antifouling strategy at the triple interface.

We chose two common ionic surfactants with identical, 12-carbon aliphatic tails to investigate the effect of surfactant charge on biofilm formation: SDS and DTAC (Figure 1). The counterions for SDS and DTAC are Na⁺ and Cl⁻, respectively, both of which are common species in bacteria culture media and thus unlikely to affect biofilm growth.

As a proof-of-principle, the concentration of surfactants was chosen to be 0.1 mM in the antifouling tests on four distinct surface chemistries to unravel the effect of surfactant charge

Figure 1. Chemical structure of DTAC and SDS.

and surface properties on biofilm formation. That concentration corresponds to 26.4 ppm for DTAC (equivalent to 0.7% of its CMC) and 28.8 ppm for SDS (equivalent to 1.5% of its CMC). The concentration was chosen based on the known fact that a dilute solution of surfactants (below 10% of its CMC) is required in order to form a monolayer at the liquid-solid interface, the adsorption behavior of which is responsive to the surface properties (e.g., charge, polarity). 23,27 As the concentration of surfactants increases to close to the CMC, surfactants tend to form hemimicelle structures with greater likelihood of antimicrobial effects at the triple interface, potentially masking the antifouling effect of the dynamic surface. Furthermore, the surfactant concentration of 0.1 mM is unlikely to affect the growth of planktonic bacteria [the minimum inhibitory concentration (MIC) is around 100 ppm for SDS and DTAC],²⁸ allowing the examination of biofilm formation without the interference from planktonic growth variability.

To systematically investigate the effect of surfactant—surface interactions on biofilm formation at the triple interface, we compared four types of surface chemistries: the pristine culture plates made of polyvinyl chloride (PVC), and functional polymer coatings made of PPFDA, PHEMA, and a polypyridine-based sulfobetaine, i.e. a zwitterionic polymer (ZWP). Those four polymer chemistries were chosen to represent the range of surface properties commonly seen in applications ranging from fabrics and biomedical devices to energy storage and manufacturing instruments. The effects of their surface energy, charge, and functional moieties on surfactant—surface interactions and subsequent biofilm formation are analyzed in detail below.

The all-dry synthetic approach, namely initiated chemical vapor deposition (iCVD), was employed for the three aforementioned functional polymer coatings to ensure parallelism. iCVD is an all-dry polymerization technique where vaporized monomers deposit and polymerize into a conformal polymer coating on substrates maintained at room temperature. The iCVD technique was chosen because it is chemically versatile and substrate independent. The solventfree nature of the technique ensures its simultaneous compatibility for the synthesis of superhydrophilic and superhydrophobic polymers. Using iCVD, surface chemistry could be varied without affecting the surface morphology, improving the validity of comparisons drawn in this study. Its substrate-independence further enables the application of functional polymer coatings to the variety of apparatuses used in the culture of biofilms.

During the iCVD process, polymer coatings were created via the following mechanisms (Figure 2): (i) introduction of vaporized monomers, carrier gas (not shown in Figure 2 due to its chemical inertness), and initiator, *tert*-butylperoxide (TBPO), into a vacuum chamber where substrates to be coated were placed on a stage maintained at room temperature; (ii) physisorption of the monomers onto the temperature-controlled substrates; (iii) formation of free radicals by the thermal decomposition of TBPO upon passing through an array of metal filaments, resistively heated to ~200–300 °C; (iv) free-radical polymerization of the surface-adsorbed monomers following an Eley–Rideal mechanism.³² The sulfobetaine-based ZWP was created using a two-step method reported in our previous work,³³ where the nitrogen in poly(4-vinylpyridine-*co*-divinylbenzene) (synthesized using iCVD)

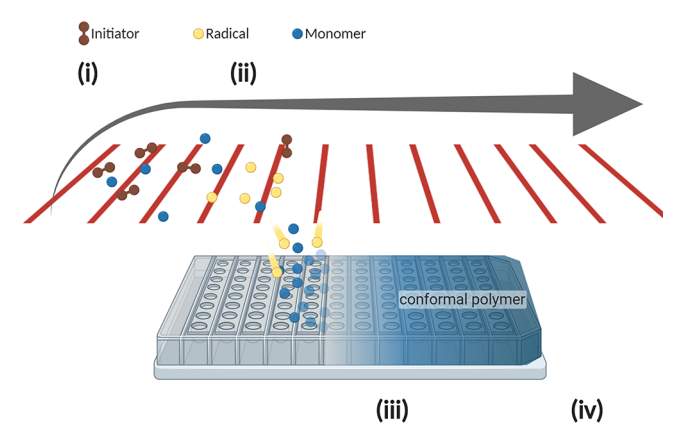


Figure 2. Schematic of the iCVD technology. (i) introduction of vaporized monomers, carrier gas and initiators; (ii) formation of free radicals by passing the initiator molecules through the heated filament; (iii) physisorption of monomers on the cooled substrate; and (iv) free-radical polymerization of the adsorbed monomers to form functional polymer thin films. Created with BioRender.com.

was converted to a quaternary ammonium group in a vaporbased derivatization step following iCVD.

Compared with other CVD polymerization techniques, a main advantage of iCVD is its conformality on substrates with high aspect ratios (as high as 275). Therefore, a conformal coating is expected on 96-well plate (aspect ratio: 1.8) using iCVD. Uniform substrate temperature could further ensure a high degree of conformality on the 96-well plates used in biofilm culture, which was achieved using custom-designed aluminum cooling block that conformed to the shape of the plate bottom. The polymer thickness was controlled to be 600 nm (measured on a Si wafer) to ensure the coverage on the culture plates by a continuous polymer film, while minimizing the impact on the overall well volume.

Molecular structures of the as-deposited polymers were confirmed using Fourier transform infrared (FTIR, Figure 3a) and X-ray photoelectron spectroscopy (XPS) (Figure 3b-d). In the FTIR spectrum of PPFDA, the peak at 1740 cm⁻¹ corresponds to C=O stretching. The peaks at 1200 and 1150 cm⁻¹ correspond to C-F stretching. The C=O and -OH bonds in PHEMA were confirmed by the 1730 cm⁻¹ peak and the broad absorption at ~3500 cm⁻¹, respectively. Successful obtainment of the sulfobetaine zwitterionic moieties in ZWP was confirmed by the 1037 cm⁻¹ peak, which is attributed to the symmetric stretching of the SO₃⁻ group. Their XPS spectra further confirmed the correct chemical makeup of the iCVD polymers, consistent with published data. The XPS highresolution scan was performed on the nitrogen atom (instead of the carbon atoms) for ZWP (Figure 3b) because the quaternary ammonium group is more indicative of successful synthesis of sulfobetaine. Upon the vapor-phase derivatization, the binding energy of N(1s) shifted from 399.5 eV (corresponding to the pyridine nitrogen) to 401.5 eV (corresponding to the quaternary nitrogen in sulfobetaine), confirming successful conversion. The XPS high-resolution carbon scans of PHEMA (Figure 3c) revealed five distinct chemical environments, corresponding to the C=O, C-O-C, C-OH, C(CH₃), and -CH₂- bonds respectively (from the Gaussian-function-based peak deconvolution). Similarly, the five different carbon environments in PPFDA (Figure 3d) correspond to CF₃, CF₂, C=O, C-O, and C-C bonds. Finally, XPS survey scans of the four surface chemistries

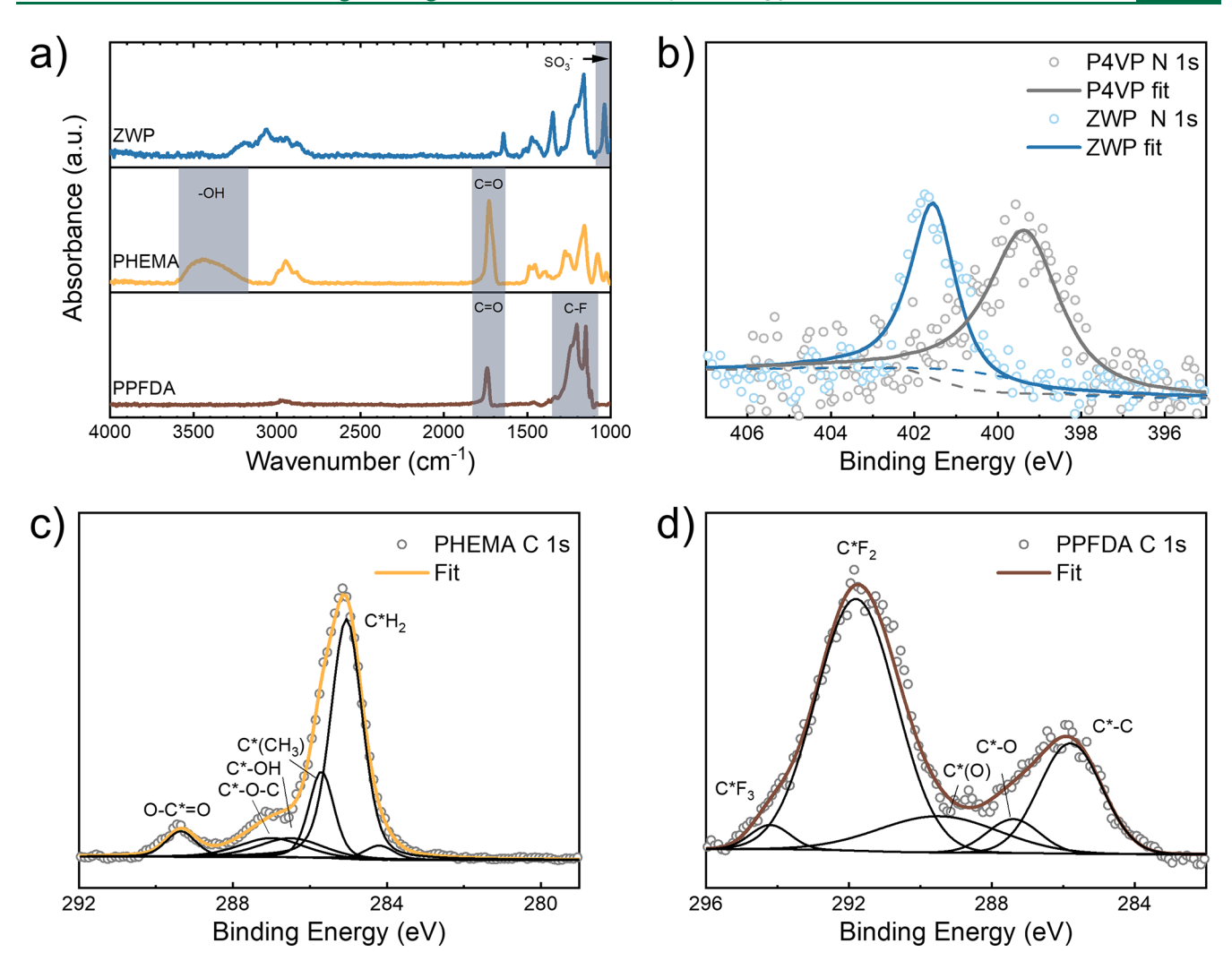


Figure 3. Confirmation of the chemical structures of the as-deposited polymers. (a) FTIR spectra of ZWP, PHEMA, and PPFDA obtained using iCVD. (b) High-resolution XPS N(1s) scans of ZWP and P4VP-co-DVB. After the vapor-phase derivatization using 1,3-propane sultone, the pyridine N became quaternized. (c) High-resolution XPS C(1s) scan of the iCVD PHEMA. (d) High-resolution XPS C(1s) scan of the iCVD PPFDA.

confirmed the elemental presence of C and Cl in PVC, C, O, and F in PPFDA, C and O in PHEMA, and C, N, O, and S in the ZWP (Figure S1). The trace amount of Si detected in the survey scan was a result of the underlying silicon wafer substrate used in the XPS analyses.

The contact angle of water was measured on those four surfaces to quantify their respective surface energies. Consistent with the literature, PPFDA exhibited a highly hydrophobic surface with a water contact angle of 119.4 \pm 0.5°, whereas ZWP was the most hydrophilic surface a water contact angle of 4.4 \pm 0.6° (Figure 4).33,35 PHEMA and PVC demonstrated intermediate water contact angles of 47.7 \pm 0.3° and 75.5 \pm 0.3° respectively, also comparable to values reported in the literature. 39,40

Biofilm growth at the triple interface was evaluated using *P. aeruginosa*, strain PAO1, due to its tendency to form biofilm at the triple interface.⁴¹ Biofilms of PAO1 have been shown to grow abundantly at the triple interface, while submerged surfaces at which only solid—liquid interface exists displays negligible growth (Figure S2).⁴² The amount of biofilm formed at the air—liquid—solid interface correlated well with the surface energy, with the least amount of biofilm on the

ZWP and most on PPFDA (Figure 4). Biofilm growth at the triple interface was evaluated using *P. aeruginosa*, strain PAO1, due to its tendency to form biofilm at the triple interface. Growth of *P. aeruginosa* and its quantification were performed using the well-established O'Toole protocol. In the absence of surfactants, PPFDA demonstrated the most biofilm growth, ~1.7-fold that on uncoated PVC culture plates; whereas the antifouling sulfobetaine chemistry, ZWP, reduced biofilm by ~3.5-fold compared to PVC. Biofilm growth on PHEMA was similar to that on PVC, which could be a result of their similar surface energies as revealed by the water contact angle measurements.

Upon introduction of 0.1 mM SDS or DTAC, biofilm growth at the triple interface was reduced universally on all four surfaces (Figure 5a), with greater effect obtained using DTAC than SDS (Table 1). On PPFDA, SDS led to a 1.7-fold reduction in biofilm formation whereas DTAC led to a 2.2-fold reduction. That comparable effect was likely a result of the charge-neutral and noninteractive nature of the highly fluorinated chemistry. Slightly greater antifouling effect was observed on PVC, with SDS and DTAC causing 2.8-fold and 3.3-fold reductions, respectively. The similar effect from SDS

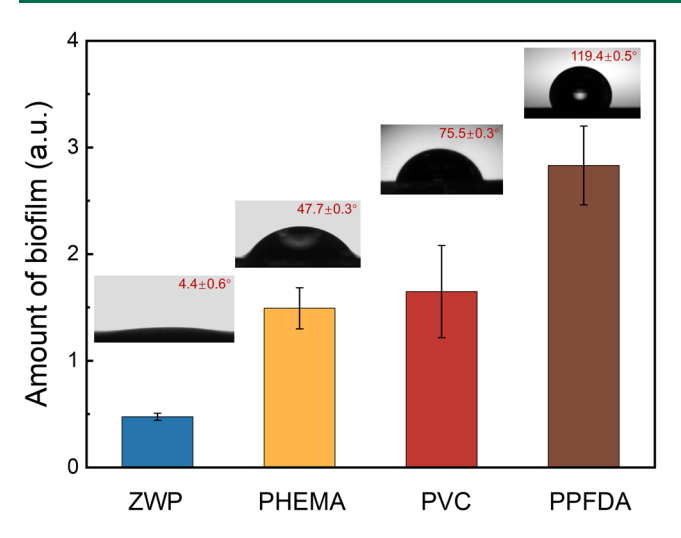


Figure 4. Water contact angle and its effect on biofilm formation. Colored columns indicate the amount of biofilm formed at the triple interface on each surface chemistry (i.e., ZWP, PHEMA, PVC, and PPFDA), quantified using the crystal violet staining method (absorption at 570 nm), after incubating PAO1 in LB medium for 24 h. Insets represent the water contact angle on each surface chemistry. Biofilm formation data are mean \pm SD (n = 5).

and DTAC was attributed to the charge neutrality of PVC, whereas the slightly greater reduction compared to those on the PPFDA surface was likely a result of the stronger dipole—dipole interactions between the surfactants and PVC. Notably, the antifouling performance of PVC in the presence of 0.1 mM DTAC or SDS was comparable to that of ZWP, a gold standard in antifouling polymers.⁴⁵

On PHEMA, DTAC led to much greater biofilm reduction (10.2-fold) than SDS (3.6-fold). A similar trend was observed on ZWP, with a 1.0-fold reduction from SDS (i.e., unchanged performance with or without 0.1 mM SDS) and 5.4-fold reduction from DTAC. For PHEMA and ZWP, the disparate effects of SDS and DTAC were attributed to the varying strength of electrostatic interactions between the surfactant and the surface. According to the literature, PHEMA has a surface zeta potential of around $-20~{\rm mV},^{46-48}$ which could be attributed to the slight deprotonation of the hydroxyl group (with the p $K_{\rm a}$ of $\sim 11-12$) under neutral pH. The zeta potential of the iCVD ZWP has been measured to be around $-13~{\rm mV}$ (Figure S2, albeit under different ionic strength from those used in biofilm culture). The negative zeta potential of

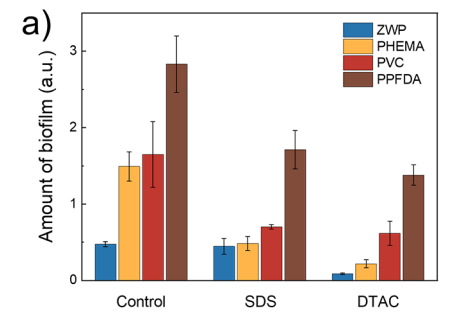
Table 1. Reduction of Biofilm Formation in the Presence of 0.1 Mm Sds or 0.1 Mm Dtac on Various Surfaces^a

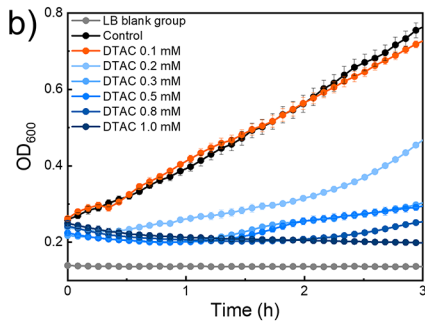
	ZWP	PHEMA	PVC	PPFDA
SDS	1.0	3.6	2.8	1.7
DTAC	5.4	10.2	3.3	2.2

^aReduction was calculated as the ratio of the amount of biofilm in the absence of surfactants to that in the presence of surfactants at 0.1 mM; biofilms were quantified using the crystal violet staining method and indicated by the reading of OD_{570} .

ZWP could be attributed to the strong acidity of the sulfonate group combined with the weak basicity of the pyridinium group. Consequently, under neutral pH, the degree of deprotonation of the sulfonate groups exceeds that of protonation of the pyridine groups, causing an overall negative charge on the ZWP surface.⁴⁹ The negative charge led to stronger surfactant—surface interactions with the cationic surfactant DTAC compared to the anionic surfactant SDS.

The observed universal reduction of the triple-interface biofilm formation on all four surfaces was a result of the surface-adsorbed surfactants, rather than the changes to the medium (e.g., pH values) or the antimicrobial effect due to the surfactants. To prove that, we measured the pH value of the medium containing different concentration of SDS or DTAC while monitoring the planktonic bacteria growth rates (Figure S3, Figure 5b, c). The pH value of the LB medium was 6.85 without surfactants and increased slightly to the range of 6.88 to 6.91 with different concentrations of DTAC or SDS. That insignificant change in pH values was unlikely to contribute to the reduction of biofilm formation. At the concentration of 0.1 mM, DTAC led to a similar growth curve as that for the control group (i.e., with no addition of surfactants), the difference between which was within experimental error. Increasing the concentration of DTAC to 0.2 mM reduced cell growth considerably, implying antimicrobial activities. That effect increased with the concentration of DTAC and at the concentration of 1.0 mM, bacterial growth was completely inhibited. That strong antimicrobial effect has been attributed to DTAC's positive charge, causing cell lysis via strong interactions with the negatively charged cell membrane.⁵⁰ By comparison, antimicrobial effect of the anionic surfactant SDS was much weaker, with no discernible difference compared to the control group up to an SDS concentration of 0.3 mM (Figure 5c). At the concentration of 0.5 mM, a sudden drop in OD₆₀₀ was observed after 2 h of incubation, indicating





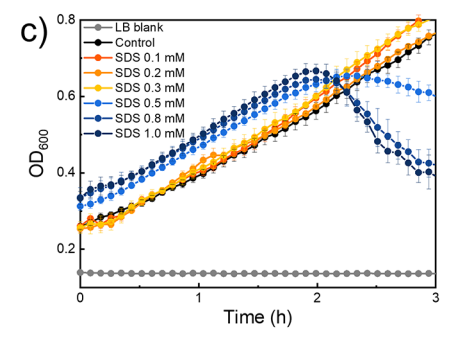


Figure 5. Reduced biofilm formation at the triple interface in the presence of surfactants. a) Colored columns indicate the amount of biofilm formed at the triple interface on each surface chemistry (i.e., ZWP, PHEMA, PVC, and PPFDA), quantified using the crystal violet staining method (absorption at 570 nm), after incubating PAO1 in LB medium for 24 h. (b, c) Planktonic PAO1 growth curves in LB medium with varying concentrations of DTAC (b) or SDS (c). PAO1 was cultured to $OD_{600} = 0.20$ before addition of surfactants. Data are mean \pm SD (n = 5).

inhibited bacterial growth. Nevertheless, the complete inhibition (like the case for DTAC at 1.0 mM) was not observed for SDS even at concentrations as high as 1.0 mM. Therefore, planktonic growth of *P. aeruginosa* was unaffected by SDS or DTAC at the employed concentration of 0.1 mM. Nevertheless, concentration of the surfactant molecules at the liquid—solid interface could still be greater than that in the bulk solution at concentrations below the CMC, potentially leading to antimicrobial effects at the surface.

To demonstrate that the reduced biofilm formation in the presence of 0.1 mM surfactants was not caused by surface-initiated antimicrobial effects, biofilms formed at the triple interface were analyzed using a live/dead assay (Figure 6).

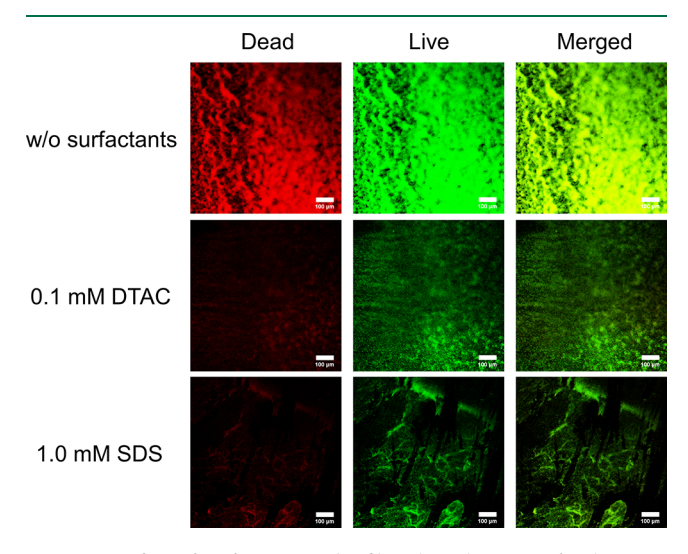


Figure 6. Effect of surfactants on biofilm physiology. Confocal images of the PAO1 biofilm (stained using LIVE/DEAD Baclight Bacterial Viability Kit; $850 \times 850~\mu m$) after incubation in the presence of 0.1 mM DTAC and 1.0 mM SDS for 24 h, where red indicates dead bacteria and green live bacteria. The merged images represent the superposition of the live and dead bacteria. Scale bar, $100~\mu m$.

After 24 h of incubation on a glass slide (required for confocal imaging) in the presence of 0.1 mM SDS or DTAC, biofilms at the triple interface were stained using a LIVE/DEAD BacLight bacterial viability kit. Confocal images of the stained biofilms were subsequently taken to assess the effect of surfaceabsorbed surfactants. A glass surface was used in the assessment of antimicrobial effects for two reasons. It provided an estimation of the upper bound of the antimicrobial effect possibly induced by the surfactants due to the strong negative charge of glass (whose zeta potential is approximately -50 mV).51 The surface negative charge led to enhanced surface adsorption of cationic surfactants, thereby corresponding to a greater potential for antimicrobial effect at the surface than any of the polymers reported here. Furthermore, glass remains the standard surface used in microbiology research and confocal imaging, the use of which enabled the direct comparison of the results reported here with the literature values. 52,53 The ratio of live to dead bacteria in the biofilm remained unchanged at the DTAC concentration of 0.1 mM compared to the surfactantfree control group, where green and red fluorescence indicated live and dead cells, respectively. At the SDS concentration of 0.1 mM, the surface of the glass slide was free of biofilm (Figure S3). Upon increasing the concentration of SDS to 1.0 mM, a majority of the bacteria in the biofilm remained alive, consistent with the established resistance of biofilm to antimicrobial agents.4 It is therefore reasonable to believe that biofilm growth was unaffected by the presence of SDS at 0.1 mM (i.e., 10% of the concentration of SDS in Figure 6).

Surfactants have been shown to lead to ECM degradation by solubilizing the adhesive components in the ECM. S4 Instead of killing the bacteria residing within a biofilm, the surface-adsorbed surfactants were shown to erode the structural integrity of the extracellular matrix, as illustrated using scanning electron microscope (SEM). SEM provided submicron-level resolution of the biofilms formed on the four surfaces, with or without surfactants (Figure 7) Without surfactants, biofilm formation was observed on all four surfaces with convoluted extracellular matrices. Upon introducing 0.1 mM of SDS or DTAC, the extracellular matrix became porous,

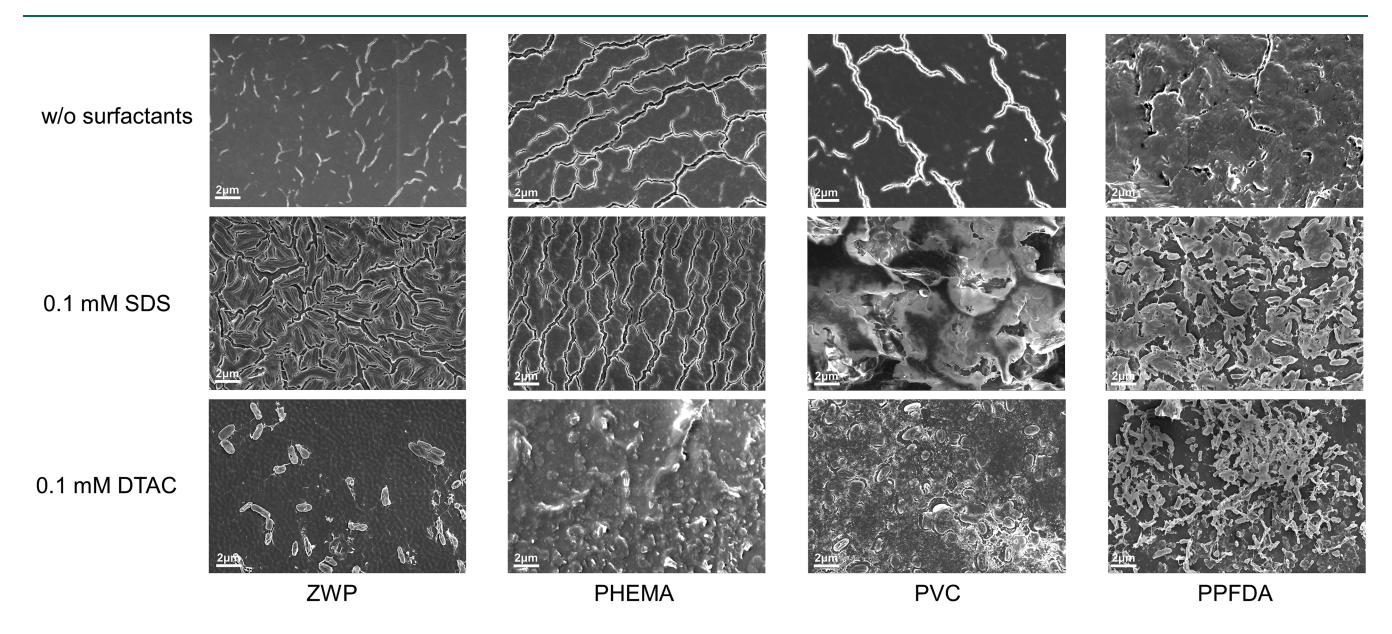


Figure 7. Combined effect of surfactants and surface properties on biofilm morphology. Representative SEM images of biofilms after incubation in the presence of SDS and DTAC (both at 0.1 mM), on various surface chemistries, for 24 h in LB medium. Scale bar, 2 μ m.

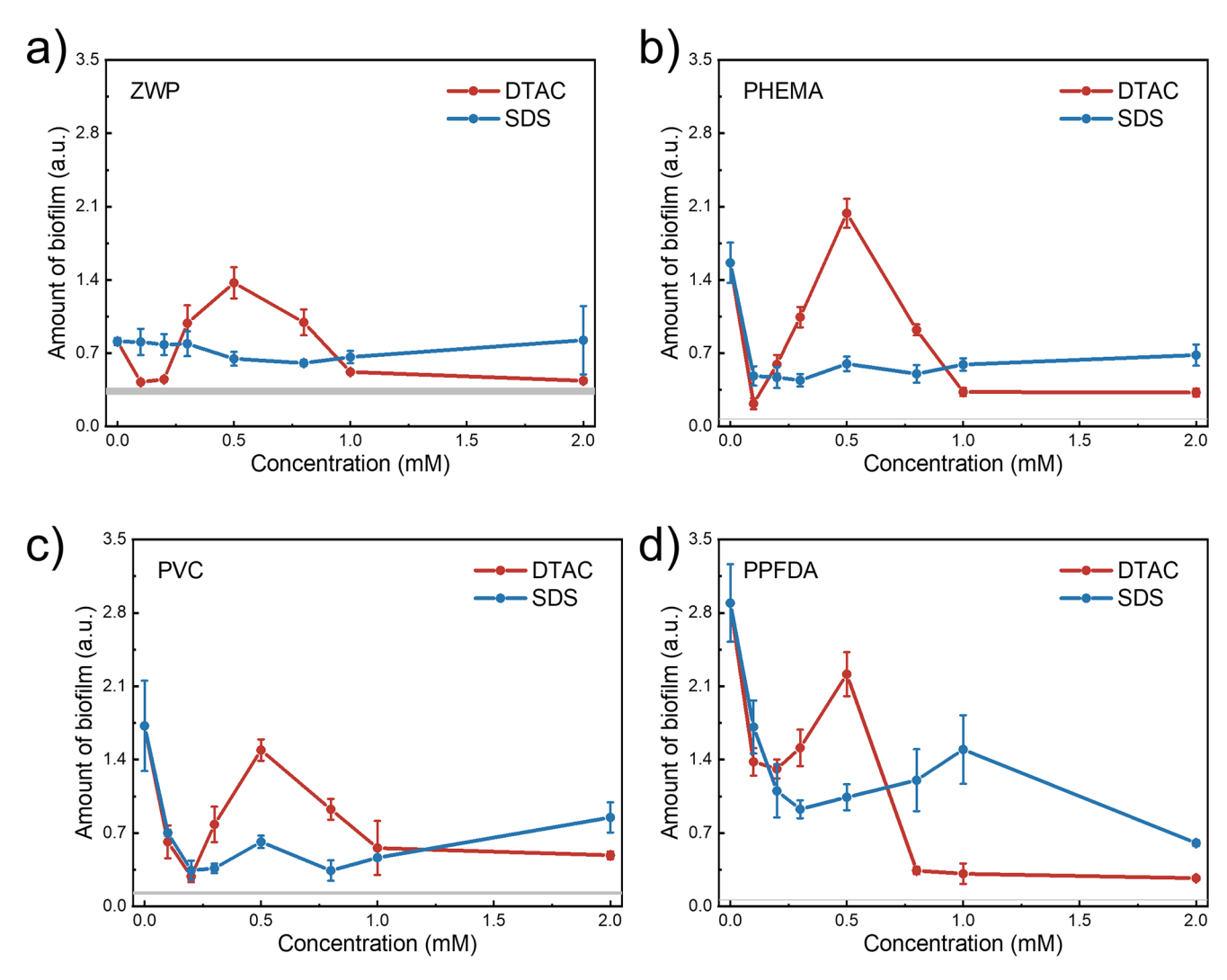


Figure 8. Biofilm formation at varying concentrations of surfactants. The amount of *PAO1* biofilm formed at the triple interface at different concentrations of DTAC or SDS, on (a) ZWP, (b) PHEMA, (c) PVC, and (d) PPFDA surfaces. Biofilm was quantified using the crystal violet staining method (absorption at 570 nm), after incubating *PAO1* in LB medium for 24 h. The gray zone in each panel indicates the OD₅₇₀ reading of a control group (i.e., no inoculation of PAO1) after the crystal violet staining treatment. Data are mean \pm SD (n = 5).

revealing the rod-shaped bacterial cells. DTAC showed a stronger effect of disrupting the extracellular matrix than SDS, which was evident from the virtually nonexistent extracellular matrices, exposing the bacterial cells on all four surfaces. The low-concentration surfactants likely reduced biofilm formation by suppression or disruption of its ECM. Although the surfactant concentrations (in the bulk solutions) required to cause ECM disruption are much greater than those used in this report (e.g., a SDS concentration of >3 mM is needed to cause ECM disruption, which is 30 times larger than the concentration used here), the polymeric surfaces likely enriched the dissolved surfactants (i.e., leading to a higher surface concentration than bulk concentration) and potentially enabled the observed ECM disruption.

Finally, the effect of surfactants at higher concentrations was studied on all four surface chemistries in search for greater resistance to biofilm formation at the triple interface (Figure 8). Upon increasing the concentration of DTAC from 0.1 to 0.3 mM, the surface accumulation of biofilm increased on all four surfaces, and that trend remained upon further increasing DTAC concentration to 0.5 mM. That was likely a result of the antimicrobial effect of DTAC, which led to cell lysis and an

increased number of surface-adsorbed biomolecules that sustained the biofilm growth. Increasing DTAC concentration to 0.8 mM reduced the biofilm growth, likely a result of the strong antimicrobial effect of DTAC. At the concentration of 1.0 mM, the amount of biofilm was reduced to close-to-zero, a result of the complete inhibition of planktonic bacterial growth (Figure 5b). The concentrations of DTAC that gave rise to the greatest resistance to biofilm formation at the triple interface were identified to be 0.1 mM for ZWP and PHEMA and 0.2 mM for PVC and PPFDA. The resulting biofilm accumulation for each case was tabulated in Table 2. SDS followed a similar trend, i.e., a slight increase in biofilm accumulation upon increasing SDS concentration to up to 0.5 mM (on PPFDA, the increasing trend continued until the concentration of 1.0 mM was reached), followed by decreasing amount of biofilm upon further increasing SDS concentration. The concentrations of SDS that led to the greatest resistance to biofilm formation were 0.8 mM for ZWP, 0.3 mM for PHEMA, 0.2 mM for PVC and 0.3 mM for PPFDA, whose resulting foldreduction in biofilm quantity was tabulated in Table 2. Notably, increasing the DTAC concentration from 0.1 to 0.2 mM enhanced the antifouling performance by 3.1-fold on

Table 2. Maximum Reduction of Biofilm Formation on Various Surfaces in the Presence of Surfactants (At Concentrations That Yielded the Maximum Reduction)^a

	ZWP	PHEMA	PVC	PPFDA
SDS	1.8 (0.8 mM)	4.0 (0.3 mM)	7.4 (0.2 mM)	3.3 (0.3 mM)
DTAC	5.4 (0.1 mM)	10.2 (0.1 mM)	10.1 (0.2 mM)	2.3 (0.2 mM)

"Reduction was calculated as the ratio of the amount of biofilm in the absence of surfactants to that in the presence of surfactants at the concentrations indicated in parentheses; biofilms were quantified using the crystal violet staining method and indicated by the reading of OD₅₇₀.

PVC. That represented a 10.1-fold reduction in biofilm quantity compared to PVC in the absence of surfactants, highlighting the effectiveness of this facile approach. Similar enhancement was observed upon increasing the SDS concentration from 0.1 to 0.2 mM, which led to a 2.7-fold reduction in biofilm quantity, corresponding to a 7.4-fold reduction compared to PVC with no surfactant.

The enhanced antifouling performance likely originated from the surface adsorption of surfactants rather than the changes in bulk properties (e.g., changes in film swelling) caused by the addition of surfactants. The surfactant solutions likely had negligible effects on the swelling of the hydrophobic polymer PPFDA and the cross-linked ZWP due to their known resistance to swelling. 5,55-58 Surfactants like SDS have been shown to increase the swelling of PHEMA gels,⁵⁹ likely a result of the hydrophobic interactions between the surfactant tail and the hydrophobic segments of the polymer (e.g., hydrocarbon backbone). 60 Although similar effects of surfactants could occur to the PHEMA thin films reported here, it was unlikely a main reason for the reduced biofilm formation caused by surfactants. That was because biofilm formation was known to correlate stronger with surface properties (e.g., interfacial energy) than bulk properties (e.g., swelling).⁶¹ Nevertheless, surfactant-mediated film swelling will be an important subject of our further explorations.

To analyze the effect of the surfactants on the coating morphology in the context of biofilm formation, the polymer coatings were exposed (for 24 h) to PAO1 cultures containing 1.0 mM SDS or DTAC. Subsequently, SEM images of the treated polymer coatings were taken at locations away from the triple interface (where biofilms tend to accumulate), enabling the direct assessment of the effect of surfactants on coating morphology under biofilm growth conditions while avoiding the interference of biofilms.

The SEM images (Figure S6) indicated that the pristine surfaces were flat and relatively smooth and free of structural features, consistent with the previous reports on polymer thin films synthesized using iCVD. 5,58 After the aforementioned treatment with PAO1 cultures containing 1.0 mM SDS, the ZWP surfaces remained unchanged, likely a result of the inherent antifouling property of the ZWP under submerged conditions.⁵ The roughness increased on the PHEMA, PVC, and PPFDA surfaces treated by SDS-containing cultures. The post-treatment roughness of the surfaces increased with their hydrophobicity, where ZWP exhibited the smallest roughness and PPFDA exhibited the largest roughness. That change in morphology was thus contributed to the bacteria growth in the presence of 1.0 mM of SDS that led to the biosynthesis and subsequent surface adsorption of biomolecules. The morphology of PHEMA, PVC, and PPFDA remained unchanged after

the treatment by DTAC-containing cultures because of the strong antimicrobial effect of 1.0 mM of DTAC, which led to complete eradication of bacteria growth. Therefore, the effect of surfactants on the surface morphology was insignificant, as indicated by the unchanged surface morphology before and after the DTAC treatment. The changes in surface roughness caused by the treatment with 1.0 mM SDS could be attributed to the accumulation of biomolecules as a result of the bacteria growth in the presence of SDS.

Nevertheless, the surface-adsorbed surfactants likely have biological effects that are beyond the quantity of biofilm formed at the air—liquid—solid interface. Unraveling the effect of surfactants and surface chemistry on the physiology of bacteria and biofilms will be a major focus of our future studies.

CONCLUSION

We introduce a facile strategy to reduce biofilm formation at the air—liquid—solid triple interface by adding trace amounts of surfactants (at 0.1 mM) to the liquid culture. Biofilm formation on the common PVC material was reduced by as much as 10.1-fold at the DTAC concentration of 0.2 mM. To unravel the mechanisms that led to the notable fouling reduction, we used the all-dry iCVD technique to fabricate surfaces with different hydrophilicity, charge, and functional moieties relevant to antifouling applications. Furthermore, two surfactants with identical hydrophobic tails (i.e., SDS and DTAC) were used to illustrate the effect of surfactant charge on biofilm formation at the triple interface.

With those surfaces (i.e., uncoated PVC and coatings of ZWP, PHEMA, and PPFDA) and the surfactants, biofilm formation was evaluated systematically. On all four surfaces, greater reduction of biofilm formation was achieved by DTAC than SDS. Among the surface chemistries, the slightly negatively charged PHEMA and ZWP yielded the greatest fouling reduction by 10.2- and 5.4-fold respectively compared to the control group where no surfactant was added. That was a notable achievement provided that PHEMA and ZWP have been used as antifouling materials, and further enhancement of their antifouling performance by as much as 10-fold was unprecedented. We attributed that considerable biofilm reduction to the dynamic interactions between surfactants and surfaces. The surfactant layer at the fluid-solid interface could adopt disparate configurations in response to the wetting state of the solid, exposing hydrophilic head groups in an aqueous environment and hydrophobic tails under ambient conditions. That dynamic behavior enabled surface hydrophilicity underwater and hydrophobicity in air for optimal fouling resistance at the triple interface.

We demonstrated that the excellent antifouling performance did not come from the antimicrobial effects of the surfactants on planktonic cells or biofilms. Instead, the biofilms, on all four surfaces, adopted a porous morphology in the presence of surfactants, implying that disrupting the extracellular matrix could be a reason for the reduced biofilm formation.

By increasing the concentration of surfactants, antifouling performance was further improved on all four surfaces. That enhancement was most significant on uncoated PVC. achieving 7.4- and 10.1-fold reduction of biofilm formation in the presence of SDS and DTAC respectively at 0.2 mM.

In summary, application of trace-amounts of surfactants led to considerable reduction in biofilm formation at the air liquid—solid interface, which was attributed to the dynamic

1

behavior of surface-adsorbed surfactant molecules. The facile strategy could be broadly adopted in antibiofouling applications, reducing contamination, energy consumption, and material degradation in areas including membrane separation, food industry, and healthcare.

ASSOCIATED CONTENT

5 Supporting Information

The Supporting Information is available free of charge at https://pubs.acs.org/doi/10.1021/acsbiomaterials.0c01691.

XPS scans, images of *PAO1* biofilms, pH values at different surfactant concentrations, zeta potential distribution graph and measurement conditions, confocal images, and surface morphology (PDF)

AUTHOR INFORMATION

Corresponding Author

Rong Yang — Smith School of Chemical & Biomolecular Engineering, Cornell University, Ithaca, New York 14853, United States; orcid.org/0000-0001-6427-026X; Email: ryang@cornell.edu

Authors

Pengyu Chen — Smith School of Chemical & Biomolecular Engineering, Cornell University, Ithaca, New York 14853, United States

Jiayan Lang — Smith School of Chemical & Biomolecular Engineering, Cornell University, Ithaca, New York 14853, United States; ⊚ orcid.org/0000-0002-0865-2690

Trevor Donadt — Smith School of Chemical & Biomolecular Engineering, Cornell University, Ithaca, New York 14853, United States

Zichen Yu — Smith School of Chemical & Biomolecular Engineering, Cornell University, Ithaca, New York 14853, United States

Complete contact information is available at: https://pubs.acs.org/10.1021/acsbiomaterials.0c01691

Notes

The authors declare no competing financial interest.

ACKNOWLEDGMENTS

The authors thank the Department of the Navy, Office of Naval Research, for support under the ONR award N00014-20-1-2418. Analytical methods involved use of the Cornell Center for Materials Research (CCMR) Shared Facilities, which are supported through the NSF MRSEC program (DMR-1719875). We thank John Grazul from the CCMR for assistance with preparation of biofilms for SEM.

REFERENCES

- (1) Farkas, A.; Song, S.; Degiuli, N.; Martić, I.; Demirel, Y. K. Impact of biofilm on the ship propulsion characteristics and the speed reduction. *Ocean Eng.* **2020**, *199*, 107033.
- (2) Ch'ng, J.-H.; Chong, K. K. L.; Lam, L. N.; Wong, J. J.; Kline, K. A. Biofilm-associated infection by enterococci. *Nat. Rev. Microbiol.* **2019**, *17* (2), 82–94.
- (3) Sadekuzzaman, M.; Yang, S.; Mizan, M. F. R.; Ha, S. D. Current and Recent Advanced Strategies for Combating Biofilms. *Compr. Rev. Food Sci. Food Saf.* **2015**, *14* (4), 491–509.
- (4) Donadt, T. B.; Yang, R. Vapor-Deposited Biointerfaces and Bacteria: An Evolving Conversation. *ACS Biomater. Sci. Eng.* **2020**, *6*, 182.

- (5) Yang, R.; Goktekin, E.; Gleason, K. K. Zwitterionic Antifouling Coatings for the Purification of High-Salinity Shale Gas Produced Water. *Langmuir* **2015**, *31* (43), 11895–11903.
- (6) Medrano-Félix, J. A.; Chaidez, C.; Mena, K. D.; Soto-Galindo, M. d. S.; Castro-Del Campo, N. Characterization of biofilm formation by Salmonella enterica at the air-liquid interface in aquatic environments. *Environ. Monit. Assess.* **2018**, *190* (4), 221.
- (7) Amara, I.; Miled, W.; Slama, R. B.; Ladhari, N. Antifouling processes and toxicity effects of antifouling paints on marine environment. A review. *Environ. Toxicol. Pharmacol.* **2018**, *57*, 115–130
- (8) Schoenitz, M.; Grundemann, L.; Augustin, W.; Scholl, S. Fouling in microstructured devices: a review. *Chem. Commun.* **2015**, *51* (39), 8213–8228.
- (9) Ganesh, V. A.; Raut, H. K.; Nair, A. S.; Ramakrishna, S. A review on self-cleaning coatings. *J. Mater. Chem.* **2011**, 21 (41), 16304–16322
- (10) Rosen, M. J.; Kunjappu, J. T. Adsorption of Surface-Active Agents at Interfaces: The Electrical Double Layer. *In Surfactants and Interfacial Phenomena* **2012**, 39–122.
- (11) Rosen, M. J.; Kunjappu, J. T. Wetting and Its Modification by Surfactants. In Surfactants and Interfacial Phenomena 2012, 272-307.
- (12) Rosen, M. J.; Kunjappu, J. T. Micelle Formation by Surfactants. *In Surfactants and Interfacial Phenomena* **2012**, 123–201.
- (13) Wu, S.; Liang, F.; Hu, D.; Li, H.; Yang, W.; Zhu, Q. Determining the Critical Micelle Concentration of Surfactants by a Simple and Fast Titration Method. *Anal. Chem.* **2020**, 92 (6), 4259–4265.
- (14) Zamfir, M.; Rodriguez-Emmenegger, C.; Bauer, S.; Barner, L.; Rosenhahn, A.; Barner-Kowollik, C. Controlled growth of protein resistant PHEMA brushes via S-RAFT polymerization. *J. Mater. Chem. B* **2013**, *1* (44), 6027–6034.
- (15) Rabin, N.; Zheng, Y.; Opoku-Temeng, C.; Du, Y.; Bonsu, E.; Sintim, H. O. Agents that inhibit bacterial biofilm formation. *Future Med. Chem.* **2015**, 7 (5), 647–671.
- (16) Wei, T.; Yu, Q.; Chen, H. Responsive and Synergistic Antibacterial Coatings: Fighting against Bacteria in a Smart and Effective Way. Adv. Healthcare Mater. 2019, 8 (3), 1801381.
- (17) Powell, L. C.; Pritchard, M. F.; Ferguson, E. L.; Powell, K. A.; Patel, S. U.; Rye, P. D.; Sakellakou, S.-M.; Buurma, N. J.; Brilliant, C. D.; Copping, J. M.; Menzies, G. E.; Lewis, P. D.; Hill, K. E.; Thomas, D. W. Targeted disruption of the extracellular polymeric network of Pseudomonas aeruginosa biofilms by alginate oligosaccharides. *npj Biofilms Microbiomes* **2018**, *4* (1), 13.
- (18) He, J.; Hwang, G.; Liu, Y.; Gao, L.; Kilpatrick-Liverman, L.; Santarpia, P.; Zhou, X.; Koo, H. l-Arginine Modifies the Exopolysaccharide Matrix and Thwarts Streptococcus mutans Outgrowth within Mixed-Species Oral Biofilms. *J. Bacteriol.* **2016**, *198* (19), 2651–2661.
- (19) DiGiandomenico, A.; Warrener, P.; Hamilton, M.; Guillard, S.; Ravn, P.; Minter, R.; Camara, M. M.; Venkatraman, V.; Macgill, R. S.; Lin, J.; Wang, Q.; Keller, A. E.; Bonnell, J. C.; Tomich, M.; Jermutus, L.; McCarthy, M. P.; Melnick, D. A.; Suzich, J. A.; Stover, C. K. Identification of broadly protective human antibodies to Pseudomonas aeruginosa exopolysaccharide Psl by phenotypic screening. *J. Exp. Med.* 2012, 209 (7), 1273–1287.
- (20) Fulaz, S.; Vitale, S.; Quinn, L.; Casey, E. Nanoparticle—Biofilm Interactions: The Role of the EPS Matrix. *Trends Microbiol.* **2019**, 27 (11), 915–926.
- (21) Nakata, K.; Tsuchido, T.; Matsumura, Y. Antimicrobial cationic surfactant, cetyltrimethylammonium bromide, induces superoxide stress in Escherichia coli cells. *J. Appl. Microbiol.* **2011**, *110* (2), 568–579.
- (22) Otzen, D. E. Biosurfactants and surfactants interacting with membranes and proteins: Same but different? *Biochim. Biophys. Acta, Biomembr.* **2017**, 1859 (4), 639–649.
- (23) Zhu, B.-Y.; Gu, T. Surfactant adsorption at solid-liquid interfaces. Adv. Colloid Interface Sci. 1991, 37 (1), 1–32.

- (24) Grosse, I.; Estel, K. Thin surfactant layers at the solid interface. *Colloid Polym. Sci.* **2000**, 278 (10), 1000–1006.
- (25) Ferrari, M.; Ravera, F.; Viviani, M.; Liggieri, L. Characterization of surfactant aggregates at solid—liquid surfaces by atomic force microscopy. *Colloids Surf.*, A **2004**, 249 (1), 63–67.
- (26) Miller, R.; Aksenenko, E. V.; Liggieri, L.; Ravera, F.; Ferrari, M.; Fainerman, V. B. Effect of the Reorientation of Oxyethylated Alcohol Molecules within the Surface Layer on Equilibrium and Dynamic Surface Pressure. *Langmuir* **1999**, *15* (4), 1328–1336.
- (27) Zhang, J.; Meng, Y.; Tian, Y.; Zhang, X. Effect of concentration and addition of ions on the adsorption of sodium dodecyl sulfate on stainless steel surface in aqueous solutions. *Colloids Surf., A* **2015**, 484, 408–415.
- (28) Li, L.; Molin, S.; Yang, L.; Ndoni, S. Sodium Dodecyl Sulfate (SDS)-Loaded Nanoporous Polymer as Anti-Biofilm Surface Coating Material. *Int. J. Mol. Sci.* **2013**, *14* (2), 3050.
- (29) Damodaran, V. B.; Murthy, N. S. Bio-inspired strategies for designing antifouling biomaterials. *Biomater. Res.* **2016**, 20 (1), 18.
- (30) Epstein, A. K.; Wong, T.-S.; Belisle, R. A.; Boggs, E. M.; Aizenberg, J. Liquid-infused structured surfaces with exceptional anti-biofouling performance. *Proc. Natl. Acad. Sci. U. S. A.* **2012**, *109* (33), 13182.
- (31) Ravizza, M.; Giosio, D.; Henderson, A.; Hovenden, M.; Hudson, M.; Salleh, S.; Sargison, J.; Shaw, J. L.; Walker, J.; Hallegraeff, G. Light as a key driver of freshwater biofouling surface roughness in an experimental hydrocanal pipe rig. *Biofouling* **2016**, 32 (6), 685–697.
- (32) Ozaydin-Ince, G.; Gleason, K. K. Transition between kinetic and mass transfer regimes in the initiated chemical vapor deposition from ethylene glycol diacrylate. *J. Vac. Sci. Technol., A* **2009**, 27 (5), 1135–1143.
- (33) Yang, R.; Moni, P.; Gleason, K. K. Ultrathin Zwitterionic Coatings for Roughness-Independent Underwater Superoleophobicity and Gravity-Driven Oil–Water Separation. *Adv. Mater. Interfaces* **2015**, 2 (2), 1400489.
- (34) Xu, J.; Gleason, K. K. Conformal, Amine-Functionalized Thin Films by Initiated Chemical Vapor Deposition (iCVD) for Hydrolytically Stable Microfluidic Devices. *Chem. Mater.* **2010**, 22 (5), 1732–1738
- (35) Gupta, M.; Kapur, V.; Pinkerton, N. M.; Gleason, K. K. Initiated Chemical Vapor Deposition (iCVD) of Conformal Polymeric Nanocoatings for the Surface Modification of High-Aspect-Ratio Pores. *Chem. Mater.* **2008**, 20 (4), 1646–1651.
- (36) Cheng, Y.; Khlyustova, A.; Chen, P.; Yang, R. Kinetics of All-Dry Free Radical Polymerization under Nanoconfinement. *Macromolecules* **2020**, 53, 10699.
- (37) Hanak, B. W.; Hsieh, C.-Y.; Donaldson, W.; Browd, S. R.; Lau, K. K. S.; Shain, W. Reduced cell attachment to poly(2-hydroxyethyl methacrylate)-coated ventricular catheters in vitro. *J. Biomed. Mater. Res., Part B* **2018**, *106* (3), 1268–1279.
- (38) Perrotta, A.; Christian, P.; Jones, A. O. F.; Muralter, F.; Coclite, A. M. Growth Regimes of Poly(perfluorodecyl acrylate) Thin Films by Initiated Chemical Vapor Deposition. *Macromolecules* **2018**, *51* (15), 5694–5703.
- (39) Ko, Y. C.; Ratner, B. D.; Hoffman, A. S. Characterization of hydrophilic—hydrophobic polymeric surfaces by contact angle measurements. *J. Colloid Interface Sci.* **1981**, 82 (1), 25–37.
- (40) Wu, W.; Wu, J.; Kim, J.-H.; Lee, N. Y. Instantaneous room temperature bonding of a wide range of non-silicon substrates with poly(dimethylsiloxane) (PDMS) elastomer mediated by a mercaptosilane. *Lab Chip* **2015**, *15* (13), 2819–2825.
- (41) Deng, B.; Ghatak, S.; Sarkar, S.; Singh, K.; Das Ghatak, P.; Mathew-Steiner, S. S.; Roy, S.; Khanna, S.; Wozniak, D. J.; McComb, D. W.; Sen, C. K. Novel Bacterial Diversity and Fragmented eDNA Identified in Hyperbiofilm-Forming Pseudomonas aeruginosa Rugose Small Colony Variant. *iScience* 2020, 23 (2), 100827–100827.
- (42) Donadt, T. B.; Yang, R. Amphiphilic Polymer Thin Films with Enhanced Resistance to Biofilm Formation at the Solid–Liquid–Air Interface. *Adv. Mater. Interfaces* **2021**, 8 (5), 2001791.

- (43) Deng, B.; Ghatak, S.; Sarkar, S.; Singh, K.; Das Ghatak, P.; Mathew-Steiner, S. S.; Roy, S.; Khanna, S.; Wozniak, D. J.; McComb, D. W.; Sen, C. K. Novel Bacterial Diversity and Fragmented eDNA Identified in Hyperbiofilm-Forming Pseudomonas aeruginosa Rugose Small Colony Variant. *iScience* 2020, 23 (2), 100827.
- (44) O'Toole, G. A. Microtiter dish biofilm formation assay. *J. Visualized Exp.* **2011**, No. 47, 2437.
- (45) Yang, R.; Goktekin, E.; Wang, M.; Gleason, K. K. Molecular fouling resistance of zwitterionic and amphiphilic initiated chemically vapor-deposited (iCVD) thin films. *J. Biomater. Sci., Polym. Ed.* **2014**, 25 (14–15), 1687–1702.
- (46) Khorasani, M. T.; Mirzadeh, H. Effect of oxygen plasma treatment on surface charge and wettability of PVC blood bag—In vitro assay. *Radiat. Phys. Chem.* **2007**, *76* (6), 1011–1016.
- (47) Gupta, M. K.; Bajpai, J.; Bajpai, A. K., Preparation and characterizations of superparamagnetic iron oxide-embedded poly(2-hydroxyethyl methacrylate) nanocarriers. *J. Appl. Polym. Sci.* **2014**, 131 (18), DOI: 10.1002/app.40791.
- (48) Son, H. S.; Kim, K. H.; Song, J. H.; Lee, W.; Kim, J. H.; Yoon, K. H.; Lee, Y. S.; Paik, H.-j. Enhanced shear thickening of polystyrene-poly(acrylamide) and polystyrene-poly(HEMA) particles. *Colloid Polym. Sci.* **2019**, 297 (1), 95–105.
- (49) Ibrahim, G. P. S.; Isloor, A. M.; Inamuddin Asiri, A. M.; Ismail, N.; Ismail, A. F.; Ashraf, G. M. Novel, one-step synthesis of zwitterionic polymer nanoparticles via distillation-precipitation polymerization and its application for dye removal membrane. *Sci. Rep.* 2017, 7 (1), 15889.
- (50) Kautz, M. J. M.; Dvorzhinskiy, A.; Frye, J. G.; Stevenson, N.; Herson, D. S. Pathogenicity of dodecyltrimethylammonium chlorideresistant Salmonella enterica. *Appl. Environ. Microbiol.* **2013**, 79 (7), 2371–2376.
- (51) Hogt, A. H.; Gregonis, D. E.; Andrade, J. D.; Kim, S. W.; Dankert, J.; Feijen, J. Wettability and ζ potentials of a series of methacrylate polymers and copolymers. *J. Colloid Interface Sci.* **1985**, 106 (2), 289–298.
- (52) Reichhardt, C.; Parsek, M. R. Confocal Laser Scanning Microscopy for Analysis of Pseudomonas aeruginosa Biofilm Architecture and Matrix Localization. *Front. Microbiol.* **2019**, *10*, 677–677.
- (53) Varadarajan, A. R.; Allan, R. N.; Valentin, J. D. P.; Castañeda Ocampo, O. E.; Somerville, V.; Pietsch, F.; Buhmann, M. T.; West, J.; Skipp, P. J.; van der Mei, H. C.; Ren, Q.; Schreiber, F.; Webb, J. S.; Ahrens, C. H. An integrated model system to gain mechanistic insights into biofilm-associated antimicrobial resistance in Pseudomonas aeruginosa MPAO1. npj Biofilms Microbiomes 2020, 6 (1), 46.
- (54) Roy, R.; Tiwari, M.; Donelli, G.; Tiwari, V. Strategies for combating bacterial biofilms: A focus on anti-biofilm agents and their mechanisms of action. *Virulence* **2018**, *9* (1), 522–554.
- (55) Yang, R.; Gleason, K. K. Ultrathin Antifouling Coatings with Stable Surface Zwitterionic Functionality by Initiated Chemical Vapor Deposition (iCVD). *Langmuir* **2012**, 28 (33), 12266–12274.
- (56) Gleason, K. K. Chemically vapor deposited polymer nanolayers for rapid and controlled permeation of molecules and ions. *J. Vac. Sci. Technol., A* **2020**, 38 (2), 020801.
- (57) Tufani, A.; Ozaydin Ince, G. Protein gating by vapor deposited Janus membranes. *J. Membr. Sci.* **2019**, *575*, 126–134.
- (58) Gupta, M.; Gleason, K. K. Initiated Chemical Vapor Deposition of Poly(1H,1H,2H,2H-perfluorodecyl Acrylate) Thin Films. *Langmuir* **2006**, 22 (24), 10047–10052.
- (59) Mun, G. A.; Yermukhambetova, B. B.; Urkimbayeva, P. I.; Bakytbekov, R. B.; Irmukhametova, G. S.; Mangazbayeva, R. A.; Suleimenov, I. E. Synthesis and Characterization of Water Soluble and Water Swelling Thermo-sensitive Copolymers based on 2- Hydroxyethylacrylate and 2-Hydroxyethylmethacrylate. *AASRI Procedia* **2012**, *3*, 601–606.
- (60) Lee, C. H.; Bae, Y. C. Effect of surfactants on the swelling behaviors of thermosensitive hydrogels: applicability of the generalized Langmuir isotherm. *RSC Adv.* **2016**, *6* (105), 103811–103821.

(61) Flemming, H.-C.; Wingender, J.; Szewzyk, U.; Steinberg, P.; Rice, S. A.; Kjelleberg, S. Biofilms: an emergent form of bacterial life. *Nat. Rev. Microbiol.* **2016**, *14* (9), 563–575.